ISSN 0001-4370, Oceanology, 2011, Vol. 51, No. 3, pp. 475–489. © Pleiades Publishing, Inc., 2011.
Original Russian Text © I.F. Gablina, L.L. Demina, O.B. Dmitrenko, N.S. Os'kina, E.A. Popova, T.A. Khusid, V.V. Shilov, 2011, published in Okeanologiya, 2011, Vol. 51, No. 3, pp. 505–520.

MARINE GEOLOGY

Composition and Secondary Alterations of Microfossils in Sediments of the Ashadze-1 Hydrothermal Field (Tropical Mid-Atlantic Ridge)

I. F. Gablina[a], L. L. Demina[b], O. B. Dmitrenko[b], N. S. Os'kina[b], E. A. Popova[c], T. A. Khusid, and V. V. Shilov[d]

[a] *Geological Institute, Russian Academy of Sciences, per. Pyzhevskii 7, Moscow, 119017 Russia*
E-mail: gablina@ilran.ru
[b] *Shirshov Institute of Geology, Russian Academy of Sciences, pr. Nakhimovskii 36, Moscow, 117997 Russia*
[c] *Federal State Unitary Enterprise Gramberg All-Russia Research Institute of Geology and Mineral Resources of the World Ocean (VNIIOkeangeologiya), pr. Angliiskii. 1, St. Petersburg, 190121 Russia*
[d] *Polar Marine Geological–Prospecting Expedition, St. Petersburg, Russia*

Received September 17, 2009; in final form, December 22, 2009

Abstract—The first thorough analysis of microfossils from ore-bearing sediments of the Ashadze-1 hydrothermal field in the Mid-Atlantic Ridge sampled during cruise 26 of the R/V *Professor Logachev* in 2005 revealed the substantial influence of hydrothermal processes on the preservation of planktonic calcareous organisms, as well as on the preservation and composition of the benthic foraminifers. From the lateral and vertical distribution patterns and the secondary alterations of the microfossils, it is inferred that the main phase of the hydrothermal mineralization occurred in the Holocene. Heavy metals (Cu, Co, Cr, and Ag) were accumulated by foraminiferal tests and in their enveloping Fe–Mn crusts. The distribution of authigenic minerals replacing foraminiferal tests demonstrates local zoning related to the hydrothermal activity. There are three mineral–geochemical zones defined: the sulfide zone, the zone with an elevated Mg content, and zone of Fe–Mn crusts.

DOI: 10.1134/S0001437011030052

INTRODUCTION

Recent sediments in areas of elevated hydrothermal activity at the sea and ocean bottom have attracted the attention of marine geologists for a long time. The most complete data on metalliferous sediments may be found in the fundamental works by [3, 4, 6]. All the researchers emphasize the importance of the knowledge of the transformations in sediments related to the recent hydrothermal activity both for practical needs as a prospecting criterion and for an understanding of the processes that occur in deep environments and are inaccessible for direct observations. The extreme chemical and thermal conditions of these zones could not but influence the distribution patterns, burial, and preservation of microplanktonic and benthic fossils throughout the ocean. Nevertheless, these aspects remain poorly studied. It is known that, during their life activity, macrozoobenthic communities influenced by hydrothermal fluids accumulate chemical elements both in their soft tissues and carbonate shells [7, 8, 10, 20, 21, 23, and others]. This influence of hydrothermal processes on the accumulation of metals in biogenic carbonate sediments of the Atlantic largely composed of foraminifers and coccoliths is practically unknown.

This work is dedicated to the influence of hydrothermal processes on the taxonomic composition, distribution, preservation, and secondary alterations of microfossils in recent organogenic sediments of the Ashadze-1 hydrothermal field in the Mid-Atlantic Ridge (MAR) and the accumulation of metals in them.

THE STUDIED AREA

The Ashadze-1 field (coordinates 12°58′N, 44°51′W) 450 m × 350 m in size is located in the tropical zone of the Atlantic Ocean being extended in the latitudinal direction. It is deepest (4100–4200 m) among the recent MAR hydrothermal fields associated with ultramafics. The field is located at the foot of the western slope of the rift valley at the highly active intersection between the marginal deep-seated fault and the zone of near-latitudinal tectonic deformations. The bottom is composed of gabbroids and serpentinized peridotites. The ultramafic rocks are overlain by recent sediments.

According to the previous investigations, the thickness of the sediments in the field exceeds 3 m and is reduced to <0.5 m near the hydrothermal mounds. The ore field is represented by two orebodies and

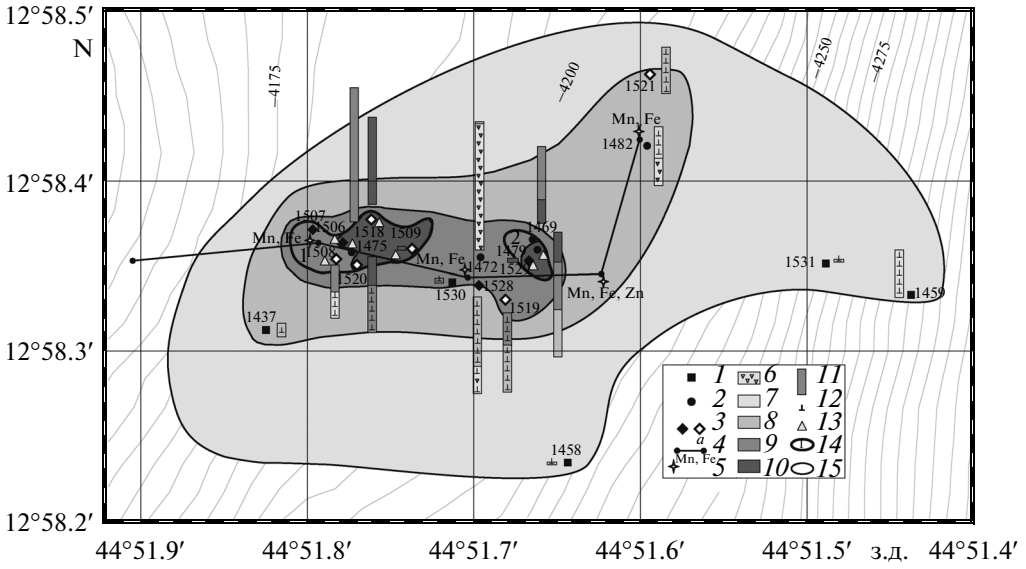

Fig. 1. The schematic distribution of the ore-bearing sediments in theAshadze-1 hydrothermal field.
(1–4) the cores and their numbers (the white and black symbols designate the original and published chemical data, respectively). (*1*) box corer; (*2*) vibrocorer; (*3*) telegreifer; (*4*) hydrophysical sonde; (*5*) geochemical anomalies in the bottom waters; (*6–10*) sediments types (according to the concentration of metals calculated for the carbonate-free matter): (*6*) metal-free (Fe < 10%, Cu+Zn < 0.25%), (*7*) metalliferous (Fe > 10%, Cu+Zn < 0.25%), (*8*) metal-bearing (Fe = 7–10%, Cu+Zn 0.25%), (*9*) ore-bearing (Fe = 10–30%, Cu+Zn *0.*25%), (*10*) ore (Fe >30%, Cu+Zn > 0.25%); (*11*) sediment cores (vertical scale 1 : 20); (*12*) carbonate; (*13*) sulfides; (*14*) contours of orebodies and their numbers; (*15*) contours of the sediment distribution areas.

includes relict and active hydrothermal vents and sediments variably enriched in metals. The sediments are classified according to the percentage of Fe, Cu, and Zn contents against the carbonate-free matter [4] (Fig. 1). The bottom water layer demonstrates anomalous turbidity, temperatures, and Fe+Mn concentrations and lowered density related to the high share of gases in the hydrothermal fluids, hydrogen and methane included [1, 13, 16]. At this field, the temperature of the fluids is as high as 353°C, the pH = 3/5 and higher, and the mineralization ranges from 0.8 to 1.3 of the seawater salinity [12]. The Th–U age of the sulfide ores from the hydrothermal mounds varies from 2.1 ± 0.3 to 7.2 ± 1.8 ka [9].

With respect to micropaleontology, the area is well studied. It is located beneath the tropical cyclonic gyre and, correspondingly, is characterized by the dominant role of tropical micro- and nannoplankton communities. The diversity of the planktonic foraminifers amounts to 20–25 species. The lysocline in the Central Atlantic is located at depths exceeding 4250–4500 m.

MATERIALS AND METHODS

We have studied the sediments sampled from the Ashadze-1 field by scientists from the Federal State Unitary Enterprise VNIIOkeangeologiya during cruise 26 of the R/V *Professor Logachev* performed by the Federal State Unitary Enterprise Polyarnaya Expeditsiya in 2005. Sediment cores were obtained by a telegreifer along the near-latitudinal profile that crosses the ore field: stations 1508, 1509, 1518, 1519, and 15121 (Fig. 1). The thickness of the recovered sediments ranges from 5 to 60 cm. They are biogenic watered mud with fragments of altered peridotites and gabbroids in the lower part. The ore-bearing and ore sediments are beige to red-brown and bluish gray in the upper and lower parts of the core sections, respectively; carbonate-free, silty–pelitic, and pelitic–gravely–sandy; frequently unsorted; and with dispersed sulfides strongly oxidized in the upper bottom layer. Metalliferous sediments are represented by beige-gray pelitic–sandy spotty carbonate and clayey–carbonate foraminiferal–nannofossil and nannofossil–forminiferal oozes [16]. According to the planktonic foraminifers, the sediments are Late Pleistocene–Holocene in age (0–30 ka) [15].

The sediments were subjected to biostratigraphic, chemical, and mineralogical analyses. The nannofossils were investigated using an Amplival biological light microscope with magnification up to 1350 and a JSM-U3 scanning electron microscope (Institute of Oceanology) with magnification up to 20000 times. The coccoliths were counted (300 specimens and more for the richest samples) under the light and scanning electron microscopes with calculation of the species' proportions (%) in the assemblages. The abundance categories were as follows: rare (single specimens in several observation fields), few (single specimens in a single observation field), common (tens of specimens in a single observation field), and abundant (hundreds of specimens in a single observation field).

The planktonic and benthic foraminifers were studied under a Leica WILD M3C light microscope at magnification up to hundreds of times. The foraminiferal tests were examined in the fractions >50 μm extracted from sediment samples of 40–60 g. Depending on the abundance, the tests were counted either in the whole residue or in its part, and then their abundance was calculated per gram of dry sediment.

The heavy metals (Fe, Zn, Co, Cr, Ni, As, Sb, Se, and Ag) in the foraminiferal tests were analyzed using the neutron activation method at the Vernadsky Institute of Geochemistry and Analytical Chemistry. The contents of Cu, Mn, Pb, Cd, and Hg were determined by the atomic absorption method (AAS) using QUANT-2A and QUANT-Z.ETA spectrometers at the Shirshov Institute of Oceanology in the flame and electrochemical variants, respectively. Because of the small quantity of matter (2–3 g), the samples of the benthic foraminifers were investigated only by the AAS method. The foraminiferal samples from two (benthic foraminifers) to 60 mg of dry weight were first decomposed in hermetic Teflon vessels in a mixture of superpure HNO_3 (1 ml) and 30% H_2O_2 (0.5 ml).

The wet chemical and atomic absorption methods were used for the chemical analysis of the sediments at the VNIIOkeanologiya enterprise; the C_{org} was determined by the Knopp method at the Geological Institute.

The mineralogical investigation of the sediments was conducted using the optical and electron microscopes (a CamScan MV2300 equipped with an INCA Energy 200 energy-dispersion analytical system at the Geological Institute). The identification of the minerals was controlled by the X-ray analysis (X-ray diffraction, Geological Institute, analyst E.V. Pokrovskaya; Debaye photomethod, Fersman Mineralogical Museum, analyst L.A. Pautov).

RESULTS

For the *biostratigraphic analysis*, samples from stations 1519, 1520, and 1521, where the organic remains are largely moderately preserved, were used. In the examined samples, they constitute up to 80–90% of the sandy and silty sediment fractions, where they are represented by planktonic and benthic foraminifers, nannofossils, ostracods, sponge spicules, and rare radiolarian specimens with planktonic foraminifers and nannofossils being dominant. Benthic foraminifers constitute only 1–2% of the total faunal abundance in the sample, or 25–30 specimens/g of the sandy fraction. The silty component of the carbonate oozes is practically entirely composed of planktonic foraminiferal tests (>99% of the total abundance); benthic foraminifers, ostracods, and sponge spicules constitute an insignificant share of the microfossils. In the samples from stations 1508 and 1518 represented by ore sediments, the organic remains are almost entirely mineralized and unidentifiable.

Nannofossils were examined in 12 samples. In total, 23 nannofossil taxa were identified; their diversity in some layers amounts to 13–14 species.

Core 1519 is composed of metalliferous and ore-bearing carbonate organogenic oozes. The upper part of the core is barren of nannofossils. In the interval of 10–50 cm, the nannofossils are well preserved and characterized by few (10–20 cm) to common (20–50 cm) total abundances (Fig. 2). The taxonomic diversity is as high as 11–14 species and is relatively constant through the section. Small nannofossils play the dominant role in the assemblage: *Emiliania huxleyi* (Lohm.) Hay, Mohl. (30–52%), *Umbilicosphaera sibogae* Weber van Bosse) Gaarder (8–23%). They are accompanied by subordinate *Helicosphaera carteri* (Wall) Kpt. (11–14%) and *Rhabdosphaera clavigera* (Murr., Blackm.) Kpt. (5–16%); slightly less abundant *Syracosphaera pulchra* Lohm. (3–9%), *Gephyrocapsa oceanica* Kpt. (4–6%), *Umbellosphaera irregularis* Paasche (2.5–6.0%), and *U. tenuis* (Kpt.) Paasche (1.5–5.0%); rare *Calcidiscus leptoporus* (Murr., Blackm.) Loebl. (0.5–3.0%) and *Oolithothus antillarum* (Cohen) Rein.; and single *Umbilicosphaera wallichi* (Lohm.) Boudr., Hay, *Scapholithus fossilis* Defl., *Ceratolithus cristatus* Kpt., *Reticulofenestra sessilis* (Lohm.) Jordan, Young, *Syracosphaera lamina* Lecal-Schlaud, and *Calciosolenia murrayi* Gran.

The lower interval (40–50 cm) contains the reworked Upper Pliocene species *Discoaster brouweri* Tan.

A similar taxonomic composition of the nannofossils is also recorded in the other examined cores.

In Core 1520 composed of carbonate-free and carbonate foraminiferal–nannofossil oozes, nannofossils were found in six layers. The upper (intervals of 0–4 and 4–15 cm) ore-bearing (4.5 and 5.63% Cu, respectively; Table 1) practically carbonate-free ($CaCO_3 < 10\%$) sediments contain single tiny poorly preserved forms. Under the electron microscope, they were identified as *Emiliania huxleyi* and *Umbilicosphaera sibogae*. The sediments from this part of the section are characterized by low $CaCO_3$ contents (4.55 and 1.15%, respectively), which increase downward to reach >25/65% (Table 1). In the interval of 25–65 cm, the abundance of the nannofossils varies from common (25–45 cm) to abundant (45–62 cm). The diversity of the assemblages ranges from 12 to 14 species. In the two lower intervals (35–45 and 45–62 cm), the abundance of the nannofossils slightly increases, and their diversity becomes as high as 13–14 species represented by *Umbellosphaea* spp., *Pontosphaera discopora* Schill., *Discosphaera tubifera* (Murr., Blackm.) Kpt., and *Ceratolithus cristatus* Kpt. The assemblage from the interval of 35–45 cm includes *Syracosphaera lamina*, which is recorded in the interval of 40–50 cm of Core 1519. The nannofossils are well preserved.

In Core 1521, the sediments are represented by organogenic mud with the $CaCO_3$ content ranging from 25.45 to 32.25%. Nannofossils were found in two intervals: 0–10 and 10–20 cm. Their total quantity

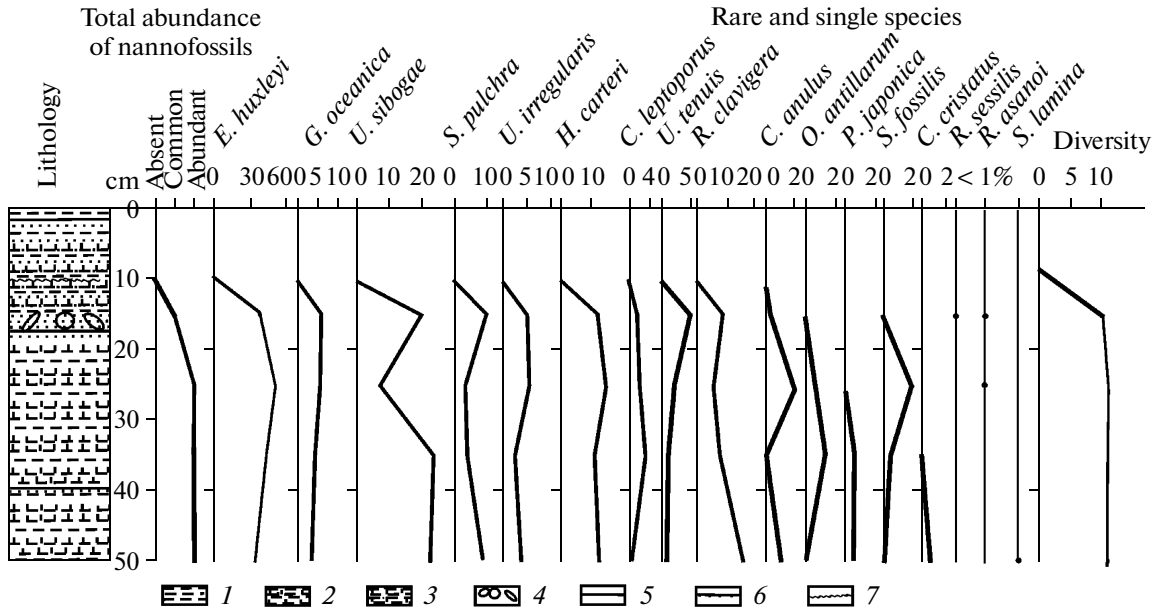

Fig. 2. The distribution of microfossils through the Core 1519 section.
(1–3) lithology: (*1*) pelite, (*2*) calcareous (foraminiferal–nannofossil) ooze, (*3*) calcareous (nannofossil–foraminiferal) ooze; (*4*) bioturbation; (*5–7*) boundaries between layers: (*5*) sharp, (*6*) gradual, (*7*) undulating.

increases downward from common to abundant, and their diversity amounts to 14 taxa in each interval. The taxonomic composition is similar to that in Core 1519. Occasionally occurring species are *Gephyrocapsa aperta* Kpt., *Reticulofenestra sessilis* in the upper interval and *Syracosphaera anthos* (Lohm.) Janin in the lower one. It should be noted that, similar to the Core 1519 section, the share of *Rhabdosphaera clavigera* increases toward the lower interval up to 15%, while that of *Pontosphaera* spp. slightly decreases in the same direction (up to 2%).

In all the examined cores, the substantial increase in the share of *Emiliania huxleyi* (from 13 to 19%) may indicate either the belonging of the host sediments to the upper nannofossil *Emiliania huxleyi* acme zone in Gartner's zonation (0–70 ka) [19] or, most likely, their Holocene age (0–11 ka). The last inference is supported by the occurrence of single *Syracosphaera lamina, S. anthos*, and *Calciosolenia murrayi*; all of them are described from recent particulate matter and planktonic samples and are rare in bottom sediments [24].

Planktonic foraminifers. These microfossils were analyzed in the sandy and silty fractions. They are well preserved, although intact tests are accompanied by their rare fragments. Almost all the examined samples contain rock clasts, which are locally ferruginate. The total abundance of planktonic foraminifers is high: up to tens and even hundreds of thousands of specimens per gram of dry sediment (Table 2).

The washed residues of the bottom sediments were divided into the following fractions: >0.5, 0.25–0.50, 0.20–0.25, 0.1–0.2, and <0.1 mm. Each of them contains 10 to 20 species of planktonic foraminifers. Their assemblages include species belonging to the equatorial–tropical, tropical, subtropical, and temperate groups with the tropical and equatorial taxa being dominant: *Globigerinoides ruber, G. sacculifer*, and *Globorotalia menardii*. It should be noted that this is true only for the coarse- and medium-grained fractions. In the finer fractions (0.1–0.2 and <0.1 mm), the foraminiferal assemblage is dominated by subtropical (*Globigerina humilis*; cores 1520-4 and 1520-5) and temperate (*G. glutinata*; cores 1521 and 1520-4) taxa. As a whole, their assemblages are characteristic of the tropical zone of the Atlantic.

The comparison of the planktonic foraminiferal assemblages in the same fraction (0.20–0.25 mm) from different intervals and different cores reveals no substantial differences. All of them are dominated by thermophilic species: tropical *Globigerinoides ruber* (up to 50%) and equatorial–tropical *G. sacculifer*. The share of each remaining species from this fraction is usually <10%.

In addition, two samples of ore-bearing sediments from Core 152 (intervals of 0–4 and 4–15 cm) were examined. It appeared that they contain only single specimens of planktonic foraminifers within the dominant inorganic mass represented by small irregularly-shaped rusty lumps. The organic component of the samples is represented by rare foraminiferal tests, their fragments, and single radiolarians. The sample from the upper interval (0–4 cm) contains an assemblage of planktonic foraminifers consisting of 20 specimens: *Globigerinoides sacculifer* (5 specimens), *G. ruber* (2), *G. conglobatus* (1), *Globorotalia tumida* (3), *G. menardii* (1), *Pulleniatina obliquiloculata* (1), *Globoquadrina duter-*

Table 1. The distribution of the main rock-forming and ore elements in the sediments of the MAR Ashadze-1 field (Fig. 1) through core sections along the NE–SW profile (% of air-dried matter)

Core	Sample (interval, cm)	SiO_2	Fe_2O_3	MgO	MnO	Al_2O_3	CaO	Cu	Zn	CO_2	S_{tot}	C_{org}
1521	1 (0–1)	14.40	4.94	3.45	0.045	3.48	33.00	0.14	0.015	28.20	0.08	0.69
	2 (1–10)	13.30	4.76	2.90	0.10	3.35	36.00	0.15	0.013	28.60	0.16	3.62
	3 (10–20)	13.35	4.53	2.30	0.10	2.91	39.50	0.13	0.012	31.66	0.16	1.09
	4 (20–30)	12.60	4.29	2.10	0.098	3.36	38.00	0.089	0.013	30.66	0.19	2.44
1529	1 (0–5)	12.3	47.78	1.14	0.06	2.68	0.49	5.36	13.59	0.37	4.71	@He опр.
1519	2 (2–10)	15.40	9.52	2.10	0.11	3.88	26.75	1.25	0.028	23.45	0.45	0.33
	3 (10–20)	11.20	5.80	1.95	0.11	3.08	36.30	0.29	0.022	29.25	0.23	0.22
	4 (20–30)	11.20	4.23	1.55	0.12	3.50	36.70	0.13	0.014	30.32	0.34	1.15
	5 (30–40)	14.20	4.16	1.80	0.11	4.58	35.00	0.1	0.014	28.66	0.19	0.32
1528	1 (0–5)	16.30	5.08	3.20	0.14	4.00	33.50	0.14	0.019	26.66	0.01	0.35
	2 (5–10)	11.30	4.27	1.40	0.10	2.95	38.50	0.16	0.020	30.80	0.32	0.26
	4 (20–30)	19.95	5.62	2.50	0.13	5.66	31.00	0.097	0.018	24.06	0.03	0.22
	6 (40–55)	26.50	6.54	11.70	0.18	5.02	20.70	0.045	0.015	16.68	0.10	≤0.1
1520	1 (0–4)	15.80	38.12	3.60	0.48	2.64	5.00	4.5	0.44	5.45	4.00	0.77
	2 (4–15)	14.60	44.23	3.60	0.70	2.62	2.12	5.63	0.33	1.56	4.50	1.31
	4 (25–35)	13.40	6.15	2.20	0.079	3.78	33.00	0.17	0.021	27.10	0.20	0.84
1518	2 (2–15)	12.20	51.48	7.62	0.009	0.54	0.49	5.55	0.38	2.18	20.27	0.12
	4 (25–35)	17.40	47.86	10.44	0.007	0.64	0.25	3.89	0.42	3.02	21.61	≤0.1
	6 (45–55)	7.40	58.14	4.64	0.019	1.14	0.29	6.54	0.13	6.50	26.75	≤0.1
1475	1 (0–20)	29.60	14.88	18.00	0.55	4.76	4.20	1.88	0.23	6.07	2.67	0.15
	2 (20–30)	30.00	14.55	18.75	0.52	4.84	4.18	1.84	0.13	6.00	2.84	≤0.1
	4 (40–50)	29.80	15.60	18.15	0.55	4.22	3.88	1.89	0.29	5.44	3.37	≤0.1
	6 (60–70)	10.80	36.46	6.04	0.11	2.54	0.95	16.30	0.91	1.15	19.23	≤0.1
	8 (80–90)	22.20	25.83	14.00	0.30	3.74	1.67	9.32	1.38	2.06	11.00	≤0.1
1508	2 (2–12)	37.10	18.27	21.80	0.14	9.63	1.17	0.28	0.058	0.45	0.36	0.20
	3 (12–22)	25.46	32.00	9.00	0.75	6.29	0.87	0.26	0.068	0.52	2.11	≤0.1
	4 (22–32)	23.64	32.60	8.88	1.42	5.50	1.22	0.097	0.016	0.62	2.16	0.26
	5 (32–45)	12.82	38.00	9.80	1.51	2.23	1.38	0.041	0.021	12.38	20.35	≤0.1
1437	1 (0–2)	11.60	4.70	2.28	0.11	3.74	35.80	0.11	0.012	28.80	0.06	0.12
	2 (2–10)	12.80	4.77	5.10	0.11	3.78	35.50	0.11	0.010	29.74	0.10	0.22

Table 2. Concentration of planktonic foraminifers, %

Ordered number	Species	Core 1519-3 (average)	Core 1519-4, fraction of 0.20–0.25 mm	Core 1519-5, fraction of 0.20–0.25 mm	Core 1520-4 (average)	Core 1520-5 (average)	Core 1521 (average)
1	*Globigerina quinqueloba*	0	0	0	0.8	0.8	0
2	*Globigerina bulloides*	0.6	0	3	0.2	0.4	1.0
3	*Neogloboquadrina pachyderma dex.*	0.3	1	1	0	0	1.7
4	*Globigerinita glutinata*	6.0	8	6	8.8	8.8	15.0
5	*Globorotalia inflata*	0	1?	0	0.4	0.4	0
6	*Globorotalia scitula*	0.3	0	0	0.8	0.6	0.7
7	*Globorotalia truncatulinoides*	1.4	1	0	0.2	0.6	1.7
8	*Globigerina falconensis*	0	0	0	0.4	0.2	0
9	*Globigerinita humilis*	1.4	0	0	14.2	8.8	0
10	*Globorotalia crassaformis*	0.3	2	7	0	0.2	2.3
11	*Globigerina calida*	0	1	0	0.4	1.6	0.7
12	*Globorotalia tumida*	1.7	0	0	0.4	1.2	0
13	*Orbulina universa*	2.0	0	0	1.8	2.2	0.7
14	*Globigerinoides ruber*	22.0	51	56	22.8	23.2	35.3
15	*Globigerinoides conglobatus*	3.3	2	0	2.8	5.4	1.3
16	*Globoquadrina dutertrei*	2.7	1	3	2.2	2.0	6.7
17	*Globigerina rubescens*	0.6	1	0	5.2	7.4	3.7
18	*Globigerinoides sacculifer*	21	18	18	18.2	18.0	18.0
19	*Globigerinella aequilateralis*	3.0	8	5	1.2	2.2	5.3
20	*Globorotalia menardii*	25.7	0	0	11.2	8.4	1.7
21	*Pulleniatina obliquilaculata*	2.3	1	0	1.0	0.4	1.0
22	*Candeina nitida*	3.3	2	0	0.8	0.6	1.3
23	*Sphaeroidinella dehiscens*	1.0	0	0	1.0	1.0	0.3
24	*Globigerina digitata*	0	2	1	0.2	2.4	0.7
25	*Globorotalia anfracta*	0	0	0	0.2	0.4	0
26	*Globigerinita iota*	0.3	0	0	2.2	2.0	0
27	*Globigerinoides tenellus*	0.3	0	0	1.2	0.8	1.0
28	*Globorotalia menardii flexuosa*	0.3	0	0	0	0.2	0
29	*Globorotalia pumilio*	0	0	0	0.4	0.4	0
30	*Hastigerina pelagica*	0	0	0	0	0.4	0
	Total	100	100	100	100	100	100

trei (5), *Globorotalia humilis* (1), and *Sphaeroidinella dehiscens* (1). In the second interval (4–15 cm), only four tests were identified: *Globigerinoides ruber, G. tenellus, Globoquadrina dutertrei*, and *Globigerina* sp. Some tests are completely enveloped by the Fe–Mn crust. All the species registered in these two layers of ore-bearing sediments were also noted in other samples (Table 2).

The planktonic foraminiferal assemblages from all the examined cores include the Quaternary index species *Globorotalia truncatulinoides*. At the same time, they are lacking species and subspecies characteristic of the Early and Middle Pleistocene, which indicates the young age of the host sediments: Holocene and, probably, terminal Late Pleistocene. None of the examined samples contains reworked older species, which implies calm sedimentation environments.

The benthic foraminifers were analyzed in the sandy and silty fractions of the metalliferous, ore-bearing, and ore sediments. In total, 49 species were identified; their distribution through the core sections is shown in Table 3.

The core sediments (two samples from Core 1520, intervals of 0–4 and 4–15 cm) contain a very impov-

Table 3. Composition and abundance of the characteristic species of benthic foraminifers (%) and ostracods (specimens/g) in the sediments of the ore field

Core	1520				1519				1521
Depth, m	4130				4173				4175
Interval, cm	0–4	4–15	25–35	35–45	10–20	20–30	30–40	40–50	1–30
Number of foraminiferal tests in the sample	11	6	3116	1482	2264	910	1696	894	2780
Abundance of foraminifers, specimens/g	4	<1	28	21	29	18	26	22	23
Diversity of foraminifers	1	2	31	26	27	24	28	27	29
Nuttalides umbonifera	11*	4*							
Quinqueloculina venusta		1*							
Nuttalides bradyi			15	14	8	11	7	27	12
Fontbotia wuellerstorfi			18	14	26	8	5	4	14
Quinqueloculina venusta + *Q. seminula*			12	17	5	20	31	6	17
Pyrgo murrhina			2	4	2	7	<1	2	2
Fissurina spp.			8	12	1	11	12	12	9
Pullenia subcarinata + *P. bulloides*			7	2	8	16	13	11	12
Globocassidulina subglobosa			15	6	3	4	13	26	8
Oridorsalis tener			2	1	0	0	2	0	4
Alabaminoides exigua			6	5	7	4	10	9	3
Alabaminella weddellensis			4	5	1.5	0	1	0	1
Gyroidina orbicularis			1	1	4.5	5	0	1	1
*Ostracod*a, specimens/g	0	0	3	7	<1	1	6	13	1

* Number of specimens in the sample.

erished benthic foraminiferal assemblage represented by two calcareous species: *Nuttallides umbonifera* and *Quinqueloculina venusta* (Table 3). In both intervals, the abundance is very low (only four specimens in the interval of 0–4 cm and <1 specimen/g of dry sediment in the interval of 4–15 cm). The tests are poorly preserved (some of them with distinct brown spots (ferrugination)). Both identified species are able to develop in bottom waters highly undersaturated with oxygen and $CaCO_3$. It is known that they tolerate almost anaerobic environments [2, 17, 18].

In the carbonate mud underlying the ore sediments, the abundance of benthic foraminifers substantially increases (up to 25–30 specimens/g) and the diversity is as high as 30 taxa. Their assemblages are dominated by calcareous porcellaneous species: *Quinqueloculina venusta, Q. seminulina*, and *Pyrgo murrhina* accompanied by other common calcareous forms such as *Fontbotia wuellerstorfi, Pullenia subcarinata, P. bulloides, Gyroidina orbicularis, Nuttallides umbonifera*, and others. Similar benthic foraminiferal communities now occupy areas covered by carbonate sediments with low organic carbon contents beneath the subtropical Atlantic gyre [11, 22]. In the assemblages from the lower parts of the core sections, the dominant role belongs to *Nuttallides umbonifera* and *Fontbotia wuellerstorfi*. The share of taxa with porcellaneous tests in these assemblages distinctly decreases.

Thus, based on the integral composition of the foraminifers and nannofossils, the sediments are dated back to the terminal Late Pleistocene–Holocene, which is consistent with the previous results by [15], who determined the age of these sediments within the limits of 0–30 ka. No reworked older species are registered in the examined samples, which implies low-energy bottom hydrodynamics during the sedimentation. The sole exception is the basal part of Core 1519, where the reworked upper Pliocene nannofossil species *Discoaster broweri* was documented.

The performed study revealed that planktonic and benthic foraminiferal assemblages are characteristic of the tropical zone of the Atlantic. No lateral changes in the distribution patterns of the nannofossils and foraminifers were noted, except for the upper layers of the cores taken from the marginal parts of orebody 1 (Core 1520) and near orebody 2 (Core 1519), where the planktonic foraminifers are characterized by poor preservation and a low abundance of identifiable tests, while nannofossils are completely or almost completely missing. The benthic foraminifers are represented by species that tolerate waters highly undersaturated with oxygen and $CaCO_3$, probably due to the influence of acid reducing hydrothermal fluids.

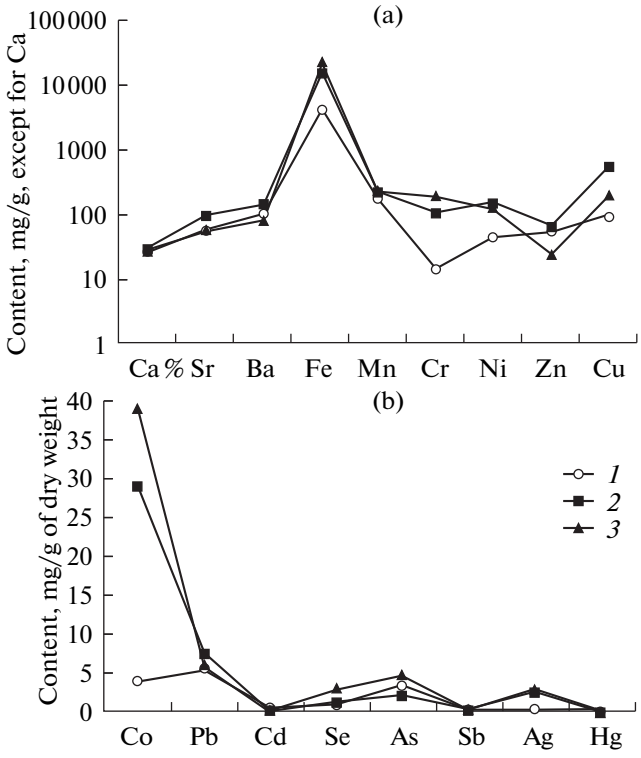

Fig. 3. Concentrations of chemical elements in tests of planktonic foraminifers (fractions <0.1 and >0.1 mm) in the Ashadze-1 field compared with the background foraminiferal values in the Central and South Atlantic.

(*1*) background, fraction >0.1 mm; (*2*) Ashadze-1 field, fraction >0/1 mm; (*3*) Ashadze-1 field, fraction <0.1 mm

(a) Ca, Sr, Ba, Fe, Mn, Cr, Ni, Zn, Cu; (b) Co, Pb,Cd, Se, As, Ag, Hg.

Downward (presumably at the Late Pleistocene–Holocene transition), the total diversities and abundances of benthic foraminifers (Table 3), nannofossils (Table 2), and ostracods increase. The abundance of the last microfossil group in the Upper Pleistocene sediments is an order of magnitude higher as compared with that in the Holocene sediments (Table 3).

Mineralogical–geochemical analysis

The chemical composition of the sediments. The performed chemical analysis of the sediments along the profile that crosses the ore field in the near-latitudinal direction reveled the zoned distribution of the rock-forming and ore elements: the contents of $CaCO_3$ and C_{org} in the sediments decrease by an order of magnitude, while the Fe, Mn, Mg, Si, and Cu concentrations sharply increase from the northeast to southwest (toward the orebody). Orebody 1 is characterized by a high Fe content in the sediments (>10–30%). Away from this orebody toward the southwestern flank of the ore field (Core 1437, Fig. 1), the $CaCO_3$ contents again increase and the concentrations of Mg and the ore components decrease (Table 1).

The accumulation of chemical elements in the microfossils. Tests of planktonic (fractions <0.1 to >0.5 mm) and benthic (fraction of 0.25–0.5 cm) foraminifers from seven and two samples, respectively, taken from the ore-bearing sediments of the Ashadze-1 hydrothermal field (Core 1520, interval of 0–5 cm) were subjected to the chemical analysis. For comparison with the background distribution of the chemical elements, nine samples of planktonic foraminifers (fraction >0.1 mm) from the bottom sediments of the Central and South Atlantic were also analyzed. Table 4 presents the results of these analyses: the Ca and Fe are given in percentage and the other elements in μg/g of dry weight. The comparison between the average concentrations of the chemical elements in the similar grain-size fractions (>01 mm) of the background planktonic foraminifers and their analogs from the hydrothermally influenced sediments of the Ashadze-1 field revealed the following features. In both cases, carbonate-forming Ca in tests of planktonic foraminifers are present in similar concentrations (Fig. 3a); moreover, this is also true of the different-size fractions. The influence of the hydrothermal fluids enriched in metals is reflected in the accumulation of metals in the tests of the planktonic foraminifers in concentrations several times higher than those observed in the tests from the background samples (Table 4). This is most notable for Fe, Ni, Co, and Cr (Fig. 3a), as well as for Co and Ag (Fig. 3b), which is determined by the elevated (relative to the other metals) contents of Fe, Cr, Ni, Co, and Ag in the fluids that circulate through the ultramafic rocks of the basement under the Ashadze-1 field. It should be noted that the Ba, Mn, Zn, Se, and Sb concentrations in the Ashadze-1 field are only slightly elevated (10–30%) relative to their background values, which, however, cannot be considered as reliably determined, as it is only slightly higher as compared with the average analytical error. The Cd, As, and Hg contents in the tests of the planktonic foraminifers of the Ashadze-1 field never exceeds that in the background samples.

No notable differences in the accumulation of most of the elements by the larger (>0.1 mm) and smaller (<0.1 mm) organisms were revealed, except for four heavy metals such as Cd, Zn, Cu, and Ni: the respective contents of the first and three last elements are twenty and three times higher in the planktonic foraminifers from the coarse-grained fractions as compared with their smaller counterparts. In the benthic foraminifers (fraction >0.1 mm), the Fe, Mn, Co, Cu, and Pb concentrations are substantially lower, while the Zn and Cd contents are higher than in the planktonic species (Table 4). The benthic foraminifers are also characterized by higher concentrations of Mn, Zn, and Cu as compared with their values in the background samples of the planktonic species. The Fe/Mn value equal to 34 in benthic foraminifers corresponds to that in the background planktonic foraminiferal samples. The insufficient data on the benthic foramin-

Table 4. Concentrations of chemical elements (Ca and Fe in %, others in μg/g of dry weight) in the tests of planktonic and benthic* foraminifers from the bottom sediments of the MAR Ashadze-1 hydrothermal field in comparison with the foraminifers from the background sediments of the central and South Atlantic

Core	Interval, cm	Fraction, mm	Ca	Sr	Ba	Fe	Mn	Co	Cr	Ni	Zn	Cu	Pb	Cd	Se	As	Sb	Ag	Hg	Fe/Mn	Fe/Mn @сред.
1520	0–5	<0.1	26.4	58	43	2.04	204	46.0	182.7	n.d	21.1	185	5.31	0.01	2.66	5.68	0.12	3.0	0.05	100	106
1520	0–4	<0.1	26.4	55	115	2.45	219	32.3	195.3	120	24.9	203	6.24	0.01	2.9	3.57	0.45	2.87	0.036	112	
1520	0–4	0.1–0.2	28.7	n.d	93	1.59	189	29.2	135.0	n.d	92.6	712	7.34	0.01	2.52	0.75	0.45	3.0	<0.01	84	84
1520	0–5	0.2–0.25	30.8	n.d	41	0.79	398	27.6	31.9	110	59.6	512	7.18	0.37	0.63	1.73	0.26	2.58	<0.01	20	
1520	0–4	0.2–0.25	29.6	n.d	29	1.33	176	21.4	61.1	50	81.7	777	9.13	0.01	0.13	5.25	0.19	2.89	0.02	74	
1520	0–4	>0.5	24.8	97	310	2.55	158	39.6	235.8	260	62.2	488	6.08	0.04	1.06	0.22	0.26	1.45	0.01	161	
1520	0–5	>0.5	31.6	n.d	220	1.55	188	27.6	38.8	190	31.6	268	8.00	0.16	1.97	2.27	0.065	2.64	0.015	82	
1520*	25–35	0.2–0.25	n.d	n.d	n.d	0.192	81.4	0.39	n.d	n.d	274	160	1.50	0.41	n.d	n.d	n.d	n.d	n.d	24	33
1521*	0–4	0.25–0.5	n.d	n.d	n.d	0.356	83.6	1.95	n.d	n.d	231	237	1.67	0.52	n.d	n.d	n.d	n.d	n.d	42	
@K-1	0–1	>0.1	31.0	n.d	245	0.47	147	3.62	5.1	n.d	13.1	30.5	7.80	0.04	0.13	7.3	n.d	0.27	0.025	32	36
3216	0–2	>0.1	2.07	115	19	0.73	93.2	7.38	73.7	100	255	172	20.32	4.72	0.66	8.36	0.6	1.36	0.246	78	
@K-5	0–1	>0.1	31.5	n.d	18	0.46	43.0	3.82	12.2	20	6.8	6.4	2.52	0.01	1.42	4.57	0.12	0.14	0.008	107	
@M-67	1–3	>0.1	n.d	n.d	n.d	1.25	239	n.d	n.d	n.d	59.0	522	6.31	0.03	í.ä.	í.ä.	í.ä.	0.37	0.025	52	
@K-1	0–1	>0.1	31.3	38	20	0.25	504	6.93	5.35	n.d	22.4	16.9	1.22	0.27	0.96	1.48	0.09	0.17	0.006	5	
@K-9	0–1	>0.1	29.6	35	305	0.2	127	0.96	7.5	50	31.2	16.1	1.68	0.19	0.23	2.15	0.25	0.12	0.014	16	
@Ш-859	0–1	>0.1	34.9	n.d	105	0.058	100	2.94	1.74	n.d	27.2	17.5	3.56	0.09	0.94	0.77	0.2	0.03	n.d	6	
4905	0–1	>0.1	33.9	n.d	61	0.19	91.7	1.76	6.86	4	48.5	37.7	1.23	0.13	3.83	2.13	0.13	0.07	n.d	21	
8106	0–1	>0.1	29.8	38	48	0.15	198	3.96	0.91	n.d	16.4	19.7	2.68	0.12	0.13	0.81	0.08	0.02	n.d	7	

Note: n.d – no data.

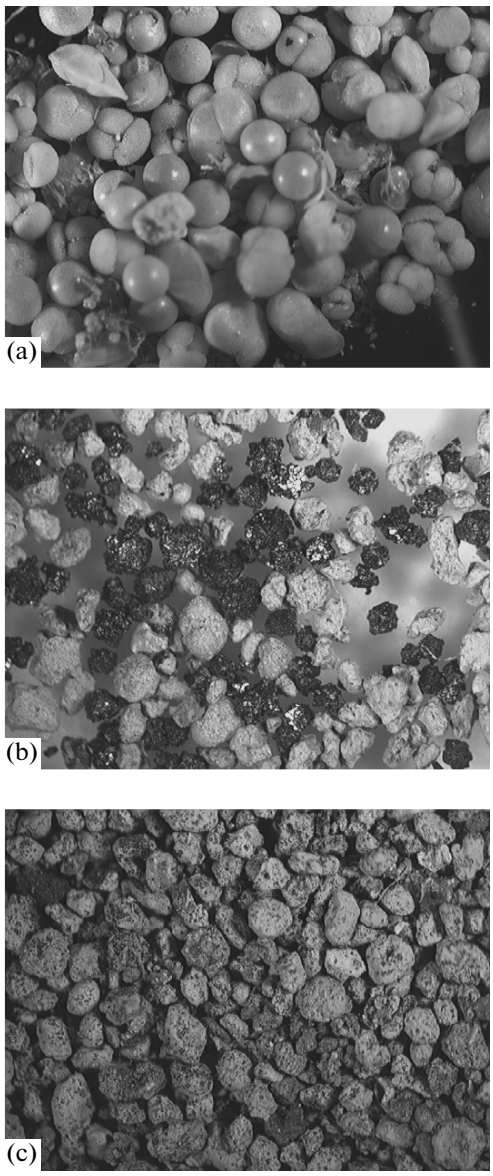

Fig. 4. General view of the variably altered foraminiferal sediments. Microimages of the fractions of 0.25–0.50 mm, 25.
(a) Core 1519, interval of 20–30 cm, slightly altered carbonate foraminiferal sediments; (b–c) Core 1508, ore sediments: (b) interval of 32–45 cm, the organogenic part is completely replaced by pyrite (black), siderite, and other hydrothermal minerals (light), (c) interval of 25–32 cm, completely replaced pseudomorphs of hydrothermal minerals after foraminifers.

ifers from the background areas prevents us from reaching a conclusion concerning the influence of the hydrothermal fluids on the accumulation of metals by their species.

The mineral composition of the microfossils. The examined samples from the ore-bearing (enriched in Fe, Cu, and Zn) layers and the ore sediments from cores 1508 and 1518 contain abundant unidentifiable organogenic structures partly or completely mineralized. By their sizes and shapes, they correspond to tests of foraminifers (Fig. 4). They were studied under the electron microscope to determine their replacing matter. For this purpose, variably altered foraminiferal tests were picked under the binocular microscope from the washed fractions of 0.20–0.25 and 0.25–0.50 mm of the sediments sampled from cores 1519, 1520, 1518, and 1508. The samples from Core 1521 do not show any alterations of the planktonic foraminifers visible under the optical microscope. For the other cores, it was established that the intensity and composition of their mineralization substantially change in the E–W direction (toward orebody 1). In the most remote (from the orebodies) Core 1519, the foraminiferal tests are practically unaltered through the entire section (50 cm), being calcite in composition (Figs. 4a, 5). Fe hydroxides and Fe–Mn films, as well as carbonaceous matter, are observable at the surface of some tests. The degree of ferrugination (limonitization?) of the tests increases in the upper bottom layer, and Fe–Mn crusts on the tests are largely observed in the lower layer.

Core 1520 recovered 55 cm of carbonate organogenic sediments with fragments of serpentinized peridotites. Samples from the upper (ore; 0–4 cm) and lower (ore-bearing; 25–35 cm) layers were examined under the electron microscope. Similar to for Core 1519, the foraminiferal tests are calcitic and sometimes with an admixture of Mg, Cu, and Si in the upper layer. The tests of the planktonic and benthic foraminifers from the lower interval are usually well preserved (Figs. 6a, 6b), while, in the upper interval, their surfaces are strongly etched and covered by a mixture of Fe hydroxides and Si with inclusions of oxidized Cu and Fe sulfides (Fig. 6c). The tests of planktonic foraminifers appear to be more intensely altered, which is likely explained by their higher porosity as compared with the benthic species. Most of the ferruginate benthic foraminiferal tests belong to the species *Valvulineria* sp., *Nuttallides umbonifera,* and *Fontbotia wuellerstorfi*, while the porcellaneous tests of *Quinqueloculina venusta* are practically unaltered or have small dissolution caverns and tiny (1–2 μm) embedded barite crystals at their surfaces (Fig. 6a).

In Core 1518 taken from orebody 1, the ore carbonate-free sediments 62 cm thick include fragments of sulfide ores and altered peridotites. The examined interval of 25–35 cm is practically barren of organogenic relicts. The sand-sized fraction of these sediments is represented by spheroid aggregates of pyrite, serpentine, and clay minerals. Their primary biogenic origin is interpreted only from their uniform sizes and spheroid shapes. The pyrite pseudomorphs are particularly difficult in their interpretation because of the intense crystallization of this mineral. At the same time, single structures preserve some features indicating their organogenic nature such as apertures, fragments of the porous surface, and two–three chambers in addition to their characteristic spheroid shape (Fig. 6d). The pyrite

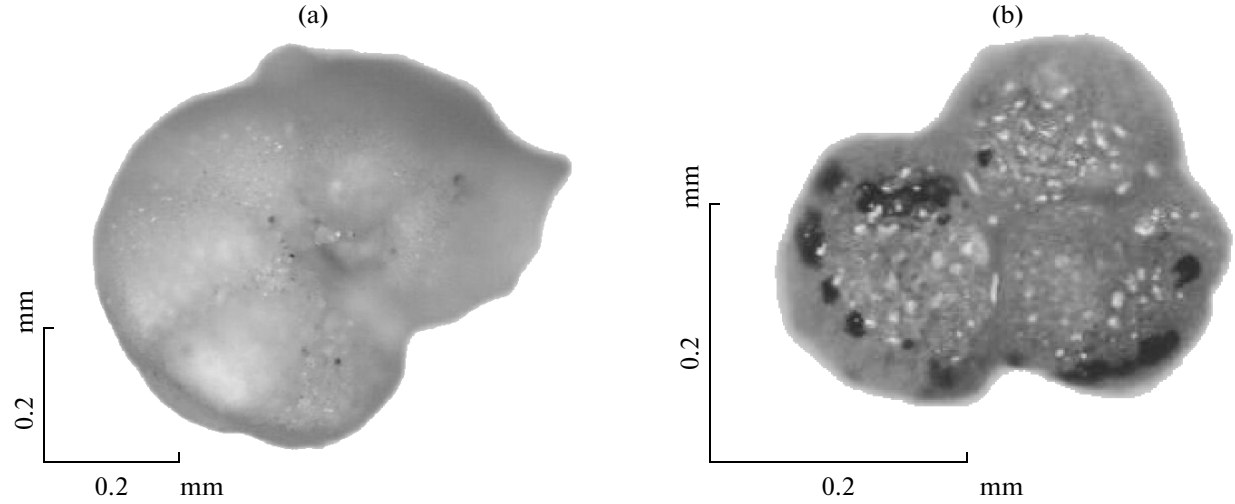

Fig. 5. Microimages of calcareous planktonic foraminifers, Core 1519, interval of 20–30 cm. The black color in Fig 6b shows the Fe–Mn crusts.

is variably oxidized and contains inclusions of Cu sulfides.

In Core 1508 located in the western periphery of orebody 1, the sediments penetrating to a depth of 45 cm are represented by carbonate-free ore-bearing pelitic–sandy (with fragments of altered peridotites) and ore mud. Samples for the analysis were taken from the upper (2–32 cm) and lower (32–45 cm) parts of the section. The detrital material from the fraction of 0.25–0.50 mm includes pseudomorphs of different minerals after tests of benthic and planktonic foraminifers and frequently with fragments of encrustation cement (Figs. 6e–6h). The authigenic minerals replacing calcite foraminiferal tests are dominated by partly oxidized pyrite and Mg–Mn-bearing siderites. In addition, the pseudomorphs after foraminiferal tests may be composed of serpentine, Mg smectite, actinolite, seladonite(?), palygorskite(?), and other minerals. The same minerals are present in the cement. Pyrite and siderite are the most widespread minerals. The latter forms fine-crystalline monomineral pseudomorphs after calcite tests and larger crystalline aggregates that cover pores in mineralized tests (Fig. 6f). The siderite includes a substantial admixture of Mg and Mn, which replace Fe in an isomorphic manner. The fine crystalline siderite that replaces the calcite tests is characterized by higher Mg (9.55–11.36%, on average 10.9%) and Mn (6.07–7.21%, on average 6.19%) contents as compared with the later siderite of the cement. In the latter, the Mg concentration ranges from 0.84 to 10.9% (averaging 7.42) and that of Mn, from 3.25 to 6.78% (averaging 4.96%). The crystalline structure of this mineral corresponds to siderite (with the strongest lines at 3.590, 2.78, 2.127, and 1.726).

Sometimes, siderite cements pyrite pseudomorphs after foraminifers.

The upper layer of Core 1508 is practically barren of relicts of organogenic structures. The residues from these sediments are dominated by spheroid grains vaguely resembling foraminiferal tests. They are largely composed of limonitized pyrite, Fe–Mg clay minerals, actinolite, Fe and Mn oxides, and other minerals (Fig. 4c).

DISCUSSION

As was shown, the hydrothermal activity in the Ashadze-1 field area substantially influenced the distribution and taxonomic composition of the micro- and nannofossils. In the Holocene sediments (0–15 cm) near the orebodies, the share of identifiable tests of planktonic and benthic foraminifers is sharply reduced (Tables 2 and 3). Nannofossils in these sediments are practically missing (Fig. 2), which is probably explained by their complete mineralization and/or dissolution by the acid hydrothermal fluids. The influence of the hydrothermal activity on the planktonic foraminifers is solely reflected in the reduced total abundance of identifiable tests because of their intense mineralization. The benthic foraminifers demonstrate a decrease in their taxonomic diversity and abundance due to the specific habitat conditions influenced by the hydrothermal fluids enriched in hydrocarbons, which create reducing H_2S-contaminated environments. Such settings determined the occurrence among the benthic foraminifers in the ore layer only species that tolerated almost anaerobic conditions (Table 3). Such a distribution and the preservation patterns of the microfossils may be used as prospecting features.

The substantial influence of the ore-saturated hydrothermal fluids is also reflected in the mineralization intensity of the foraminiferal tests. Based on the dominant minerals that cover and replace the tests, the

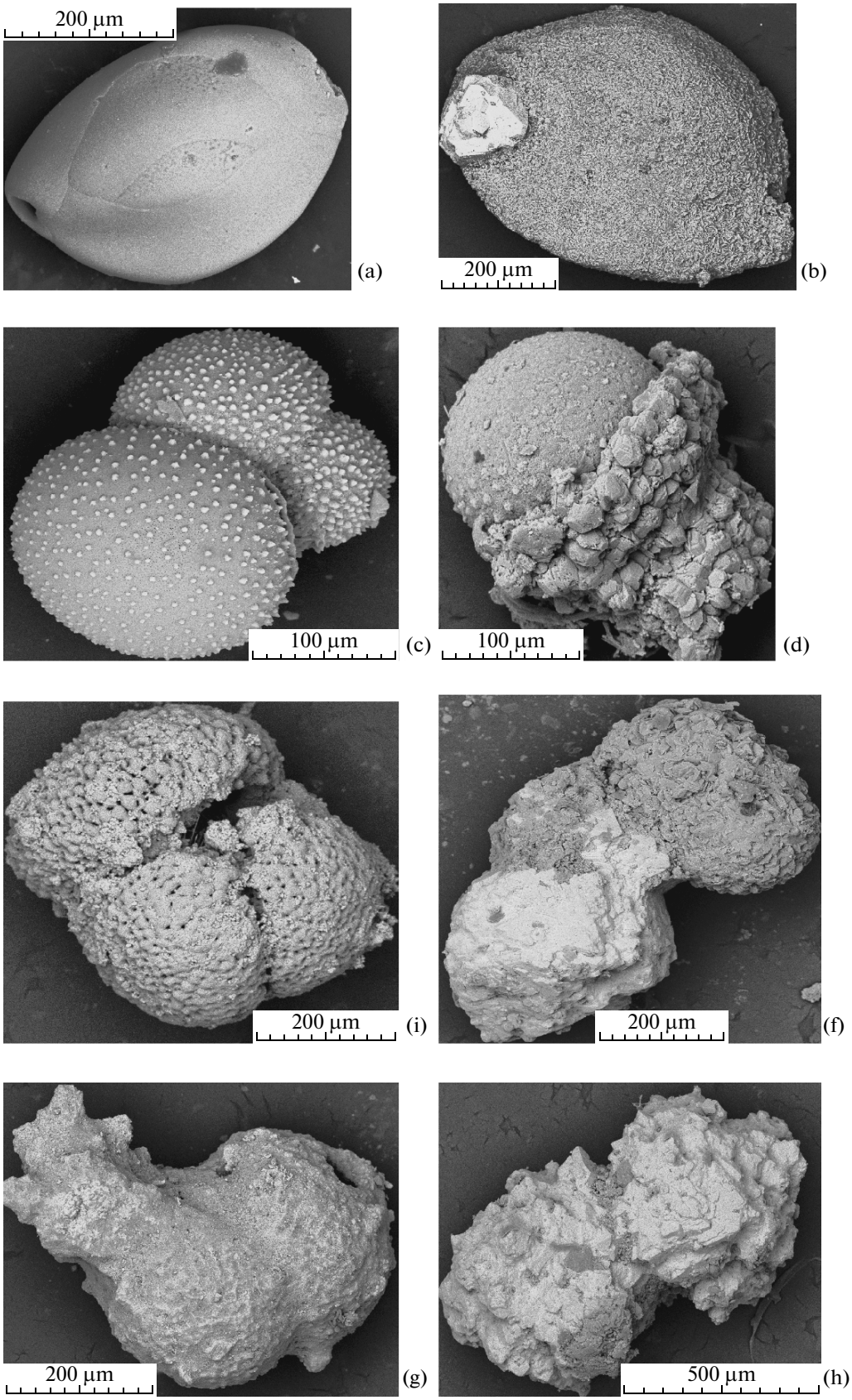
200 μm
(a)
200 μm
(b)
100 μm
(c)
100 μm
(d)
200 μm
(i)
200 μm
(f)
200 μm
(g)
500 μm
(h)

Fig. 6. Alterations in the foraminiferal tests from the organogenic ooze of the Ashadze-1 field illustrated by SEM images. The chemical composition is according to the X-ray spectral microprobe analysis.

(a, b) Core 1520, interval of 25–35 cm: (1) slightly altered test of the benthic foraminiferal species *Quinqueloculina seminulina* (Linne). The test is calcitic with an Si admixture (0.06%); the surface is covered by caverns and tiny Ba crystals; the dark spot corresponds to carbonaceous matter; (b) unaltered calcareous test of the planktonic foraminiferal species *Globigerina bulloides*; (c) Core 1520, interval of 0–4 cm; substantially dissolved and ferruginate calcareous test of *Globigerinoides conglobatus*; pores and some areas of septal sutures are filled with fine aggregate of clay minerals, SiO_2, Fe, and Cu oxides with Cu relicts; (d) Core 1518, interval of 5–35 cm; pseudomorph of strongly oxidized pyrite (an. 23–26) with inclusions of Cu sulfides (an. 27) after the two-chamber test of *Globigerinoides* sp. with relict pores and apertures; (e–h) Core 1508, interval of 53–45 cm: (e) test of the benthic foraminiferal species *Quinqueloculina seminulina* (Linne) completely replaced by fine-crystalline Mg–Mn-bearing siderite: in the aperture, a pyrite crystal, (f) test of the planktonic foraminiferal species *Orbulina universa* Orbigny completely replaced by Fe–Mn smectite (?) and submerged into crystalline–granular Mg–Mn-bearing siderite with inclusions of Fe–Mg smectite (?), (g) intergrown tests of unidentifiable foraminifers completely replaced by hydrothermal minerals; the upper part shows relicts of the two-chamber tests replaced by fine-crystalline Mg–Mn-bearing siderite, and the lower part shows a shapeless test completely replaced by pyrite submerged into the pyrite and Mg smectite cementing mass; (h) two intergrown shapeless tests completely replaced by crystalline pyrite with relict primary spherical outlines and characteristic sizes of pyritized foraminiferal tests; the pyrite contains olivine fragments (compact dark gray areas); the unconsolidated mass is composed of Mg smectite and Mg–Mn-bearing siderite with Fe oxides and Cu sulfides.

following zoning is definable in the Ashadze-1 hydrothermal field: (1) a sulfide zone corresponding to the orebody (Core 1518); (2) a zone of minerals with elevated Mg concentrations along the western and southwestern periphery of orebody 1 (Core 1508); (3) a zone of development of Fe–Mn crusts that fringe orebodies 1 and 2 (cores 1519, 1520). In the peripheral areas of the hydrothermal field under consideration (Core 1521), the dissolution and replacement of the carbonate tests by authigenic minerals fade out. The mineral zoning is also reflected in the chemical composition of the sediments.

The mineralogical–geochemical zoning defined in the sediments of the Ashadze-1 field is determined by the superposed hydrothermal processes. The zone of elevated Mg concentrations in the sediments corresponds to the distribution area of the hydrothermal sulfide ores (orebody 1) with some westward and southwestward offset relative to the sites with the maximal Fe concentrations (cores 1475 and 1508). It is known that Mg-bearing silicates (talc, chlorite, saponite, and vermiculite) in association with sulfides, silica, and anhydrite mark the areas of the hydrothermal discharge in the Red Sea [3]. It is noteworthy that Mg is also present in the hydrothermal fluids of the Red Sea (the Atlantis-II and Discovery deeps), which is untypical of oceanic hydrothermal vents usually barren of Mg [5].

A peculiar feature of the Ashadze-1 hydrothermal field is the occurrence of siderite enriched in Mg and Mn in association with Fe–Mg-bearing silicates. The wide development of high-magnesium minerals in oceanic hydrothermally altered ore-bearing and ore sediments indicates a high concentration of this mineral in the fluids that influenced the sedimentation. The occurrence of Mg in siderite is consistent with the data on its elevated content in the plume above the Ashadze-1 hydrothermal field [1, 14]. The quantitative ratios between the Fe, Mg, and Mn in the siderite of the different generations imply a progressive decrease of the Mg and Mn concentrations in the mineral-forming solutions.

As was shown by the geochemical investigations of the slightly altered calcite foraminiferal tests, the Mn content in them in the Ashadze-1 field insignificantly exceeds its background values recorded in the planktonic values from other areas of the Atlantic (only by 10–30%). The average Fe/Mn value in the background planktonic foraminifers is equal to 36, while, in the Ashadze-1 field, it is as high as106 and 84 on the average for the foraminiferal tests from the fractions <0.1 and >0.1 mm, respectively. It should be noted that a similar Fe/Mn value (81 on average) was previously obtained for Fe–Mn hydroxide crusts developed at the surface of the bivalve mollusks *Bathymodilus* from the MAR Rainbow field [8]. Fe–Mn crusts cover the foraminiferal tests along the periphery of the ore bodies. The ore bodies themselves are composed of sulfides both in ore mounds (chimneys) and in the sediments. Moreover, the sulfides in the sediments were formed owing to the dissolution of carbonate tests by acid hydrothermal fluids and their metasomatic replacement by pyrite, Cu sulfides, and other authigenic minerals. The reduced C_{org} content in the sulfide-formation zone indicates that the organic matter of the sediments, as well as the hydrocarbons from the hydrothermal fluids, took part in this process. Under such reducing conditions, the Mn hydroxides released during the dissolution of the calcite cement in the tests likely also passed into the solution, and the Mn could have subsequently precipitated in the bivalent form as the isomorphic admixture in the siderite. Along the periphery of the orebodies, where the influence of the hydrothermal fluids became reduced, Fe and Mn precipitated in the form of oxides and hydroxides covering the foraminiferal tests. Being effective sorbents, the newly formed hydroxides captured from the seawater the heavy metals (Cu, C, Cr, and Ag) supplied by the hydrothermal fluids.

Judging from the distribution and total abundance of the nannofossils and foraminifers in the examined sections, the mineralization in the Ashadze-1 field occurred only in the Holocene and negatively affected the abundance and diversity of the benthic forms,

which were solely represented by species that tolerated almost anaerobic environments. Nannofossils practically disappeared from the sediments, and the preservation of planktonic foraminifers in the upper layer of the sediments near the main orebody took place (Core 1520). It is conceivable that the accumulation of the upper sediment layer (4–15 cm) in the Holocene corresponded to the main phase of the hydrothermal activity. This inference is consistent with the data on the age estimates obtained for the hydrothermal mounds of the Ashadze-1 field ranging from 2.1 ± 0.3 to 7.2 ± 1.8 [9]. In the orebody area (cores 1508, 1518), the microfossil remains are mineralized through the entire section, which indicates the percolation of the hydrothermal fluids through the existing sediments. Moreover, it seems that that the western periphery of orebody 1 (Core 1508) was influenced by later postore Fe–Mn-enriched, although less acid, fluids, which stimulated the replacement of the calcitic foraminiferal tests with Mg–Mn-bearing siderite. The nannofossils and foraminifers in the sediments of Core 1521 located at a significant distance from the hydrothermal vents avoided their influence.

CONCLUSIONS

(1) The substantial changes in the taxonomic composition of the benthic foraminifers and the preservation of the planktonic foraminiferal tests first revealed by the thorough investigation of the hydrothermal alterations in the sediments from the Ashadze-1 field may be used as prospecting features.

(2) The lateral and vertical distributions of the microfossils indicate that the main phase of the hydrothermal ore formation corresponds to the Holocene, when the upper 15- to 20-cm-thick sedimentary layer was accumulated.

(3) The tests of planktonic foraminifers from the hydrothermal field are characterized by elevated Fe, Cu, Co, Cr, Ni, and Ag contents as compared with their counterparts in the background sediments. The substantially higher Fe/Mn values in the planktonic foraminifers, as well as the results of the mineralogical investigations, provide grounds for the assumption that the accumulation of metals in them was most likely determined by their absorption at the Fe–Mn crusts covering the surfaces of the foraminiferal tests.

(4) The local zoning in the distribution of the authigenic minerals replacing calcite in the foraminiferal tests is related to the hydrothermal activity.

(5) The zone of the elevated Mg concentrations presumably isolated in space and time from the main ore-formation zone (orebody 1) is probably related to the influence of later more Fe–Mn-enriched (although less acid) hydrothermal fluids percolating through the underlying sediments.

ACKNOWLEDGMENTS

We are grateful to our colleagues A.T. Savichev, N.V. Gor'kova, L.A. Pautov, E.V. Pokrovskaya, and M.P. Chekhovskaya for their help in the analytical studies, the sample photographing, and discussing the results. This work was supported by the Russian Foundation for Basic Research.

REFERENCES

1. V. E. Beltenev, T. V. Stepanova, V. V. Shilov, et al., "New Hydrothermal Field at 12°58.4′N and 44°51.8′W SAKh," in *Processes in a Slow-Spreading and Ultraslow-Spreading Oceanic Ridges: From Mantle Melting to the Biota in Hydrothermal Vents. Workshop of the Russian Branch of the Intrerridge International Project* (GEOKhI im. V.I.Vernadskogo, Moscow, 2003), p. 15 [in Russian].
2. I. I. Burmistrova, "The Influence of Geographical Conditions on the Quantitative Distribution of Shells of Benthic Foraminifera in the Surface Sediments in the Northern Part of the Indian Ocean," in *Marine Micropaleontology* (Nauka, Moscow, 1982), pp. 114–121 [in Russian].
3. G. Yu. Butuzova, "Hydrothermal-Sedimentary Ore Formation in the Rift Zone of the Red Sea," in *Tr. GIN RAN* (GEOS, Moscow, 1998), Vol. 508 [in Russian].
4. G. Yu. Butuzova, *Hydrothermal-Sedimentary Ore Formation in Oceans* (GEOS, Moscow, 2003) [in Russian].
5. *Hydrothermal Sulfide Ores and Metalliferous Sediments of the Ocean*, Ed. by I. S. Gramberg and A. I. Ainemer (Nedra, St. Petersburg, 1992) [in Russian].
6. E. G. Gurvich, *Metalliferous Sediments of the World Ocean* (Nauchnyi Mir, Moscow, 1998) [in Russian].
7. L. L. Demina, S. V. Galkin, A. Yu. Lein, and A. P. Lisitsyn, "First Data on Microelemental Composition of Benthic Organisms from the 9°50′N Hydrothermal Field, East Pacific Rise," Dokl. Akad. Nauk **415** (4), 528–531 (2007) [Dokl. Earth Sci. **415A** (6), 905–907 (2007)].
8. L. L. Demina and S. V. Galkin, "On the Role of Abiogenic Factors in the Bioaccumulation of Heavy Metals by the Hydrothermal Fauna of the Mid-Atlantic Ridge," Okeanologiya **48** (6), 847–860 (2008) [Oceanology **48** (6), 784–797 (2008)].
9. V. Yu. Kuznetsov, G. A. Cherkashev, V. E. Bel'tenev, et al., "The 230Th/U Dating of Sulfide Ores in the Ocean: Methodical Possibilities, Measurement Results, and Perspectives of Application," Dokl. Akad. Nauk **416** (5), 666–669 (2007) [Dokl. Earth Sci. **417** (8), 1202–1205 (2007)].
10. V. N. Lukashin, S. V. Galkin, and A. Yu. Lein, "Features of the Chemical Composition of Animals of the Deep-Sea Gidrotermal Area," Geokhimiya, No. 2, 279–285 (1990).
11. N. P. Lukashina, *Paleoceanology the North Atlantic in the Late Mesozoic and Cenozoic, and the Emergence of the Modern Global Thermohaline Conveyor According to the Study of Foraminifera* (Nauchnyi Mir, Moscow, 2008) [in Russian].

12. S. M. Sudarikov, D. V. Kaminskii, M. V. Krivitskaya, and S. S. Filatova, "Hydrothermal Fluids and Plumes of the 13°–16°N Segment of Mid-Atlantic Ridge," in *Minerals of the World Ocean-4*) (VNIIOkeangeologiya, St. Petersburg, 2008), pp. 22–25 [in Russian].

13. S. M. Sudarikov, D. V. Kaminskii, and E. V. Narkevskii,
1 "Hydrophysical and Hydrochemical Features of Hydrothermal Plumes in the Bottom Waters of the Region 12058°N SAKh," in *VI Workshop of the Russian Branch of the InterRidge International Project, June 6–7, 2009* (VNIIOkeangeologiya, St. Petersburg, 2009), pp. 55–57 [in Russian].

2 14. V. V. Shilov, V. E. Bel'tenev, and A. V. Neshcheretov, ""New Hydrothermal Ore Field 1258°4′N, 4451°8′W SAKh (Anemone Garden–Ashadze): Bottom Waters, Bottom Sediments, Igneous Rocks," in *Geology of the Seas and Oceans: Abstracts of the XV International School of Marine Geology* (GEOS, Moscow, 2003), Vol. 2, pp. 50–51 [in Russian].

3 15. V. V. Shilov, G. A. Cherkashev, V. Yu. Kuznetsov, et al., "First Data on High-Temperature Hydrothermal Activity, Which Has an Age of over 200 Kyr (SAKh, region 13°N)," in *Workshop of the Russian Branch of the InterRidge International Project* (VNIIOkeangeologiya, St. Petersburg, 2005), p. 4 [in Russian].

16. V. E. Beltenyov, Shilov V.V., E. A. Popova, and I. Rozhdestvenskaya, "Geochemical Features of Sediments at the Hydrothermal Fields of MAR 13°N," in *Minerals of the Ocean-3," Future Developments. International Conference. Absracts* (VNIIOkeangeologia, St. Petersburg, 2006), pp. 28–29.

17. M. L. Bremer and G. P. Lohmann, "Evidence for Primary Control of the Distribution of Certain Atlantic Ocean Benthonic Foraminifers by Degree of Carbonate Saturation," Deep-Sea Res. **29**, 987–988 (1982).

18. B. H. Corliss, "Microhabitats of Benthic Foraminifera within Deep-Sea Sediments," Nature **314**, 435–438 (1985).

19. S. Gartner, "Calcareous Nannofossil Stratigraphy and Revised Zonation of the Pleistocene," Mar. Micropalaeontol. **2**, 1–25 (1977).

20. E. Kadar and V. Costa, "First Reports on the Micro-Essential Metal Concentrations in Bivalve Shells from the Deep-Sea Hydrothermal Vents," J. Sea Res. **56**, 37– 44 (2006).

21. G. Roesijadi and E. A. Crecelius, "Elemental Composition of the Hydrothermal Vent Clam *Calyptogena magnifica* from the East Pacific Rise," Mar. Biol. **83** (2), 155–161 (1984).

22. D. Schnitker, "Quaternary Deep-Sea Benthic Foraminifera and Bottom Water Masses," Ann. Rev. Earth Planet. Sci. **8**, 343–370 (1980).

23. D. R. Smith and A. R. Flegal, "Elemental Concentrations of Hydrothermal Vent Organisms from the Galapagos Rift," Mar. Biol. **102**, 127–133 (1989).

24. J. R. Young, M. Geisen, L. Cros, et al., "A Guide To Extant Coccolithophore Taxonomy," J. Nannopl. Res. Spec. Issue **1**, 125 (2003).

SPELL: 1. Hydrochemical, 2. Bel'tenev, 3. Cherkashev